Automated Deep Learning Pipeline for Accurate Segmentation of Aortic Lumen and Branches in Abdominal Aortic Aneurysm: A Two-Step Approach

Fatma N. Hassan
Department of Electrical Engineering
Benha Faculty of Engineering, Benha University
Benha, Egypt
fatima.nassr@bhit.bu.edu.eg

Ahmed M. Mahmoud
Department of Biomedical Engineering and Systems
Cairo University
Giza, Egypt
Astute Imaging
Kirkland, WA 98033, US
a.ehab.mahmoud@eng1.cu.edu.eg

Ahmed F. Elnokrashy
Department of Computer Science
Technology and Computer Science, Nile University
Giza, Egypt
Benha University
Benha,Egypt
ahmed.elnokrashy@bhit.bu.edu.eg

Ashraf Y. Hassan
Department of Electrical Engineering
Benha Faculty of Engineering, Benha University
Benha, Egypt
ashraf.fahmy@bhit.bu.edu.eg

***Abstract*— Abdominal Aortic Aneurysm (AAA) is a serious medical condition characterized by the abnormal enlargement of the abdominal aorta. If left untreated, AAA can have life-threatening consequences. Accurate segmentation of the aorta in Computed Tomography Angiography (CTA) images plays a vital role in treatment planning for AAA. However, manual and semi-automatic segmentation methods suffer from limitations in terms of time and accuracy. This study presents a deep learning pipeline that aims to fully automate the precise and efficient segmentation of the aorta and its branches within CTA images. A two-step approach is proposed for the segmentation of the aorta and its branches in contrast-enhanced CTA scans. The first step involves utilizing a UNet++ model to perform aortic segmentation across the entire set of CTA axial slices. In the second step, a post processing algorithm is employed to track the continuity of the segmented aorta while effectively discarding false positive (FP) objects. The assessment of the fully automated method revealed remarkable outcomes, with a mean Dice coefficient of 0.941 on a test set consisting of 10 CTA scans. The automated segmentation results are utilized to create a comprehensive 3D model. The study results indicate that the utilization of the proposed deep learning-based pipeline is highly effective in achieving accurate segmentation of the aortic lumen and its branches. The practical implications of this approach extend to pre-operative planning. This highlights the valuable contribution of the proposed method in improving the management and treatment of patients diagnosed with aortic aneurysm.**

Keywords—Deep learning, Aorta segmentation, UNet++, Abdominal Aortic Aneurysm.

I. Introduction

Abdominal Aortic Aneurysm (AAA) is characterized by the weakening and expansion of the abdominal aorta [1]. AAA represents a significant public health concern, with varying prevalence rates across different populations. This condition contributes to approximately 1% of deaths among males aged 65 and older, resulting in over 175,000 fatalities worldwide. The mortality rate associated with aneurysm rupture is alarmingly high, estimated to be between 60% and 80%. Consequently, early detection and timely treatment play a critical role in preventing rupture and mitigating its devastating consequences [2].

In recent years, surgery has been superseded with less invasive endovascular aneurysm repair as the surgical management of abdominal aortic aneurysms (EVAR). During the intervention, the surgeon inserts one or more stent grafts into the aneurysm sac using a catheter that is inserted through an access channel, such as the femoral arteries. By reducing the aneurysm sac's pressure, EVAR lowers the chance of wall rupture [3].

The primary diagnostic imaging modality for aortic aneurysms is Computed Tomography Angiography (CTA), although ultrasound imaging is the preferred screening modality for this condition. The primary uses of CTA are in treatment planning and aneurysm progression assessment. With the aortic arch down to the femoral arteries, it offers a thorough imaging picture of the whole aorta. Reconstructing orthogonal pictures of the vessel, segmenting the aorta, and creating three-dimensional models of the aorta are all done using commercially available treatment planning software. For the purpose of EVAR planning and treatment choices, this makes it possible to assess vascular diameters, lengths, and volumes precisely [4].

During EVAR planning, accurate aortic branch segmentation is essential since it directly influences the measures needed to choose the appropriate stent graft [5]. Aortic segmentation could be labor-intensive and prone to human mistake, though. Furthermore, the degree of expertise of the readers affects the precision of aortic volume measurement made by hand segmentation [6].

When segmenting vessels using automated or semi-automatic approaches, at least one expert is needed to complete the segmentation or evaluate the accuracy of the results. The vast number of articles published each year on this subject indicates that, in spite of these difficulties, automatic or semi-automatic blood artery segmentation is a topic of great interest in medical research and has the potential to benefit physicians [7].

979-8-3503-6263-3/24/$31.00 ©2024 IEEE

De Bruijne et al. [8] presented an interactive method for separating the aneurysm sac from a dataset of CTA that included 23 patients. The method involves combining statistical understanding of object shape and changes with a local appearance model close to the object outlines. It was based on active shape model segmentation. After manually segmenting the first slice, the technique automatically finds the contour in the successive slices, allowing for quick processing of the AAA's whole volume.

Duquette et al. [9] devised a semi-automatic method to separate the AAAs' aneurysmal sac from multi-slice MRI and CT scan images using graph cut theory. This technique can segment the aortic wall and lumen interface of AAAs with little assistance from humans. It is a generic approach that operates independently on both MRI and CT-scan volumes. The technique was assessed using a dataset consisting of 10 synthetic images and 44 patients, and the segmentation and maximum diameter estimation were contrasted with four experts' hand tracing.

Deep learning methods have become extremely effective tools in the field of medical image analysis in recent years, showing exceptional results in tasks including detection, segmentation, and classification [11]. The promise of deep learning-based methods in the field of endovascular care has been notably emphasized by a number of studies.

In the study by Salvi et al. [12], the feasibility of automating the segmentation of AAAs was investigated using a 3D U-Net CNN model trained and tested on a dataset of 30 CTAs, with a focus on convergence and segmentation accuracy measured by the Dice Similarity Coefficient (DSC). Optimum probability thresholds were determined for voxel-level outputs, and 3D volume rendering was used for validation and parameter optimization.

In the work by FANTAZZINI et al. [3], the aorta in the sub-sampled CTA volume is located and coarsely segmented using a CNN. Next, three single-view CNNs are used to precisely and more finely segment the aorta lumen from the axial, sagittal, and coronal planes. Next, a spatially coherent segmentation is obtained by integrating the predictions of the three networks. In a subsequent paper published in 2022 [13], two deep learning-based methods were created to automatically partition the aortic lumen and thrombus from preoperative CTA data. Following that, the diameters of the AAAs were automatically retrieved. This work was expanded in the paper published in 2023 [14], where the greatest abdominal aortic diameter was recorded using a threshold value of 30 mm. An accurate basis for comparison was provided by a radiologist performing blinded manual measurements. 48 patients with aneurysms and 25 without underwent testing of the screening pipeline created throughout the study.

UNet++ architecture comprises an encoder and decoder, interconnected by nested dense convolutional blocks. The primary objective of UNet++ is to effectively bridge the semantic gap between the feature maps of the encoder and decoder before fusion occurs. UNet++ is a sophisticated architecture that performs better than earlier models like U-Net and broad U-Net for medical picture segmentation. Using hierarchical, dense skip pathways, this deeply-supervised encoder-decoder network bridges the semantic gap between the encoder and decoder sub-networks. When the feature mappings from the two networks are similar, the optimizer can handle a learning problem that is simpler in this way [15]. When compared to the UNet design, the UNet++ architecture performed better at the task of change detection using very high-resolution images [16]. UNet++'s performance in medical image segmentation is assessed on a range of tasks, such as liver segmentation in abdominal CT scans, nuclei segmentation in microscope images, and nodule segmentation in low-dose CT scans of the chest. According to the experimental findings, UNet++ under deep supervision outperforms U-Net and wide U-Net by an average of 3.9 and 3.4 points, respectively, in the Jaccard index [15].

Existing approaches for aortic lumen and thrombi detection and segmentation often rely on 2D CNNs and have limited applicability to specific segments of the aortic lumen or thrombosis. To address these limitations, this study introduces a novel deep learning methodology that aims to precisely locate and segment the abdominal aortic lumen, extending to the iliac arteries, while incorporating branch vessels in the abdominal segment such as the celiac, superior mesenteric artery, and left and right renal arteries, with a focus on maintaining spatial coherence. The proposed approach presents a fully automatic pipeline for aortic lumen segmentation, employing CNN to segment the entire CTA scan. Additionally, volume-of-interest selection methods are incorporated to address any potential gaps in the segmentation. The resulting automatic segmentation is utilized to generate a comprehensive 3D model, which is then rigorously evaluated by comparing it against the ground truth segmentation.

II. MATERIALS AND METHODS

We have created a comprehensive pipeline for the automated segmentation of the aorta to iliac region, as shown in Fig. 1. The pipeline encompasses three distinct stages, each serving a specific purpose. In the initial stage, we employ pre-processing techniques to adequately prepare the input data. Subsequently, we utilize the UNET++ segmentation model to perform the initial segmentation, providing an initial segmentation output. Finally, to enhance the detection of any missing branches and effectively filter out potential false positive objects, we incorporate a post processing algorithm. This algorithm plays a crucial role in refining the segmentation results. In the subsequent subsections, we will delve into each stage of the pipeline, providing a detailed explanation of their respective methodologies and contributions.

A. Dataset

This paper utilizes a publicly available multicenter aortic vessel tree database [17], comprising 56 aortas and their branches. Aortic arch, ascending aorta, head/neck region, thoracic aorta, abdominal aorta, and lower abdominal aorta with the iliac arteries branching into the legs are among the regions covered by the CTA scans in the database. A semi-automatically generated segmentation mask of the aortic artery tree, made with 3D Slicer, is included with every scan in the collection [18]. The scans originate from different collections and hospitals.

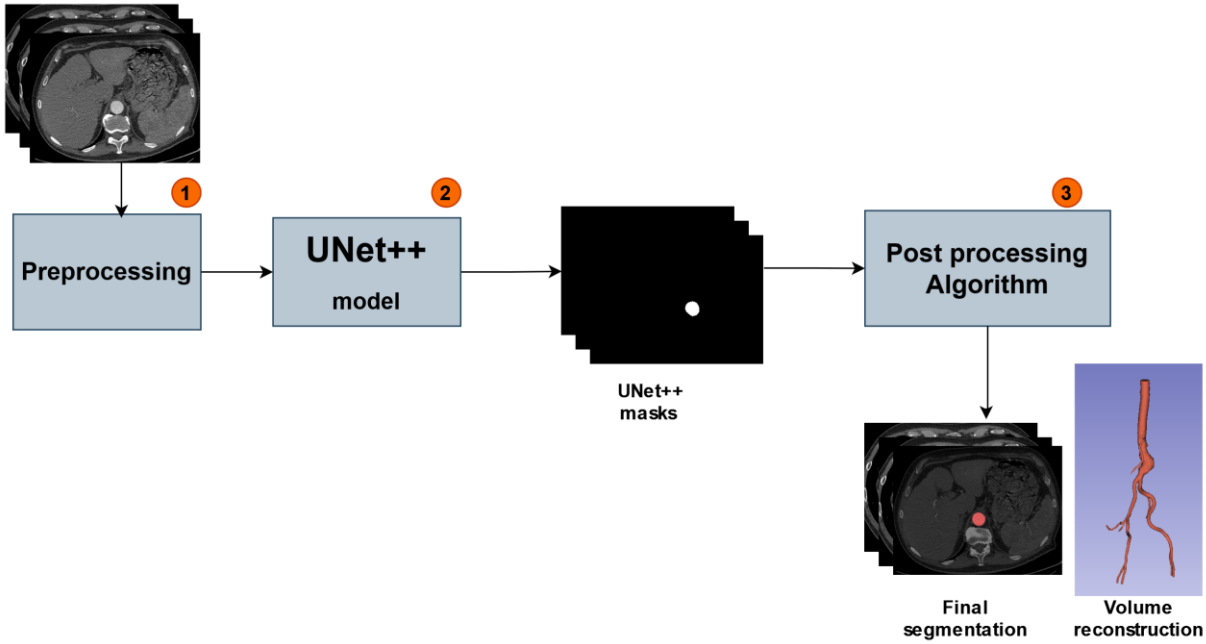

Fig. 1. Block diagram of the proposed pipeline for automatic segmentation of the aorta and its branches.

The dataset files are in nearly raw raster data format, accompanied by corresponding ground truth (GT) segmentations. The segmentations are saved using the .seg.nrrd file extension to differentiate them from the volumes, which have the .nrrd file extension. A summary of the dataset's statistics, including resolution, the number of axial slices, slice thickness, pathologies and number of cases are provided in Table 1. The number of axial slices and slice thickness are given as: min⁄median/max .

To establish a robust dataset, the CTA scans and corresponding segmentations were divided into: a training set (consisting of 41 scans) and a test set (comprising 10 scans). we started the scans from abdominal aorta.

B. *Data Preprocessing*

The subsequent sections will elaborate on the essential steps involved in data preprocessing, which is crucial for effectively training deep learning networks.

TABLE I. THE AORTIC VESSEL TREES IMAGE INFORMATION

Image Information	**KiTS**	**RIDER**	**Dongyang**
resolution	512×512	512×512	512×666
Axial slices	94/146/1059	260/1008 /1140	122/149/251
Slice thickness (mm)	0.5/5/5	0.625/0.625/ 2.5	2/3/3
Pathologies	None	AD, AAA	None
Number of Cases	20	18	18

1) Balancing small branches: Accurately segmenting the smaller branches, such as the celiac artery, superior mesenteric artery, left and right renal arteries, and iliacs, is crucial for surgical planning in cases of AAA. However, these branches often possess unique shapes that differ from the main aorta, presenting a challenge for segmentation algorithms. Furthermore, the limited number of slices containing these branches makes it difficult to obtain an adequate amount of training data for deep learning models to effectively capture the diverse morphologies. To address this challenge, we have implemented balancing by repetition. This approach involves repeating a small portion of the training images that specifically focus on these cases with smaller branches. By repeating these images, we ensure that there is sufficient representation and emphasis on the segmentation of these specific branches. In Fig. 2, we provide two example images that highlight the presence of the celiac artery in (a) and the left renal artery in (b). These images demonstrate that accurately segmenting these smaller branches needs specialized techniques, such as balancing by repetition, to improve their segmentation performance.

2) Data augmentation: In domains like medical imaging, where acquiring large datasets can be difficult, data augmentation techniques are commonly employed to increase the diversity of labeled training sets. Data augmentation has also gained popularity as an effective strategy for mitigating overfitting in deep convolutional neural networks, serving as an

implicit form of regularization [19]. The training procedure involves the application of the following augmentations:

- Shift, rotate, and scale are frequently used in medical image processing. The purpose of these augmentations is to increase data diversity and machine learning models' resilience by adjusting the size, position, and orientation of images.
- Grid distortion and elastic transform techniques have proven to be valuable in handling non-rigid structures with shape variations in medical imaging. These methods effectively address challenges associated with such structures, leading to improved image analysis and interpretation [20].
- Random brightness contrast is the process of randomly modifying an image's brightness and contrast levels. This method makes the model more adaptable to changes in lighting conditions by adding variances in the intensity values [21]. It can simulate various imaging conditions or scanner characteristics.

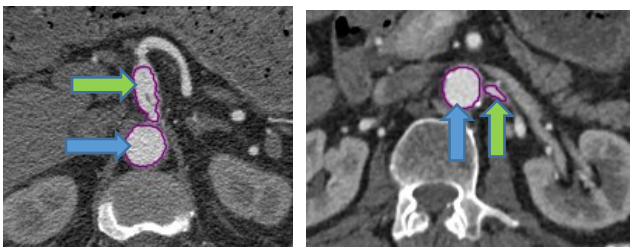

Fig. 2. Example images of irregular and small branches in the aorta (a) shows the celiac artery (green arrow) and the aortic trunk (blue arrow) in a CTA slice, and (b) describes a CTA slice including the left renal artery (green arrow) and the aortic trunk (blue arrow).

C. *UNet++ Segmentation*

For the segmentation of the aortic lumen, we employed the UNet++ architecture, fine-tuning the model with axial view of CTA images. These images had a full dynamic range of 12 bits and a resolution of 512x512 pixels. To enhance the efficiency of the network, we utilized the Xception[22] encoder, which is pretrained on the ImageNet dataset and known for its depth-wise separable convolutions.

In semantic segmentation tasks, class imbalance is a common challenge. This refers to the uneven distribution of pixels or voxels across different classes within the image. In the case of aortic lumen segmentation, the small size of the aortic region in the slice image can result in class imbalance, which can adversely impact the performance of semantic segmentation models [23]. To tackle the class imbalance issue, we implemented the Dice loss + Soft cross entropy loss function. This combination was chosen to address the imbalance problem effectively.

D. *Post Processing Algorithm*

3D spatial coherence is a crucial aspect that needs to be incorporated into the segmentation process to overcome the limitations of 2D CNNs, which often fail to capture the complete 3D structure, resulting in the omission of certain branches. To address this issue, we developed the Post processing algorithm, which takes advantage of the continuous nature of the aortic lumen on each slice. By leveraging this continuity, we can predict that instances that do not continue across slices are most likely false positive instances. Additionally, the algorithm has the capability to interpolate missing instances.

The Post processing algorithm operates as follows:

1.Starting from the bottom slice mask, each instance in the CTA slice is considered as a starting seed for a chain.

2.The algorithm determines the intersection of each instance with instances from the previous slices.

3.While the intersection with the previous instance is above a specified threshold, the current instance is considered as part of the current chain.

4.This process is repeated for each instance in the slice.

5.Chains with a length below a specified threshold (chain length threshold = 2) are filtered out as they are considered false positive instances.

6.Missing instances within each chain are interpolated to ensure a complete and continuous representation.

7.Finally, the chains are merged by combining all objects from all chains into their respective slices.

By applying the post processing algorithm, we address the limitations of 2D CNNs by taking into account the 3D spatial coherence of the aortic lumen. This enables more accurate segmentation by effectively identifying and excluding false positive instances while interpolating missing instances.

E. *Evaluation Metrics*

The following metrics were used for comparing the results of segmentation against ground truth.

1) The Dice Similarity Coefficient: Also referred to as the overlap index, the Dice coefficient (DICE) is the most often used evaluation metric in medical segmentation. The calculation for this measure is as (1) :

$$\text{Dice}=\frac{\mathbf{2}|\mathbf{S_g} \cap \mathbf{S_p}|}{|\mathbf{S_g}| + |\boldsymbol{S_p}|} \qquad (1)$$

Where Sg is the GT segmentation and Sp is the obtained segmentation.

2) The intersection over union (IOU), often known as the Jaccard index (JAC), is defined as (2):

$$\text{JAC}=\frac{|S_g \cap S_p|}{|S_g \cup S_p|}=\frac{\text{TP}}{\text{TP + FP + FN}} \qquad (2)$$

Where TP is true positives, FP false positives and FN false negatives [24].

F. Experimental Settings

The segmentation pipeline was implemented in Python, utilizing the PyTorch [25] framework with GPU support. The training and testing were conducted on a Linux Ubuntu 20.04.4 LTS 64-bit operating system. The hardware configuration included a NVIDIA GeForce RTX 3080 Ti graphics card.

III. Results

The UNet++ model was trained on axial CTA images. Some samples of UNet++ segmentation versus the ground truth for testing cases are shown in Fig. 3.

After UNet++ segmentation, the produced masks are propagated through the post processing algorithm. as shown in Fig. 4, an example of a rejected FP instance after applying the post processing algorithm. Quantitative results achieved by the UNet++ model and after the post processing algorithm are reported in Table 2, showing enhancement in average ± standard deviation Dice coefficients and JAC coefficients after using the post processing algorithm.

Fig. 5 shows the 3D models generated from the automatic and ground truth segmentations aligned together.

TABLE II. Evaluation metrices for test cases

Metric	UNet++ Segmentation (Mean ± SD)	After Post Processing Algorithm (Mean ± SD)
Dice coefficient	0.939 ± 0.054	0.941 ± 0.054
JAC index	0.892 ± 0.086	0.894 ± 0.085

IV. Discussion

In this study, we propose a deep learning approach that enables spatially coherent segmentation of the aorta to iliac arteries. Unlike previous studies that focused on a single area, our dataset includes annotations for the aorta and iliac segments, including aortic branches such as the celiac trunk, superior mesenteric artery, and renal arteries. [10],[26], [27] This

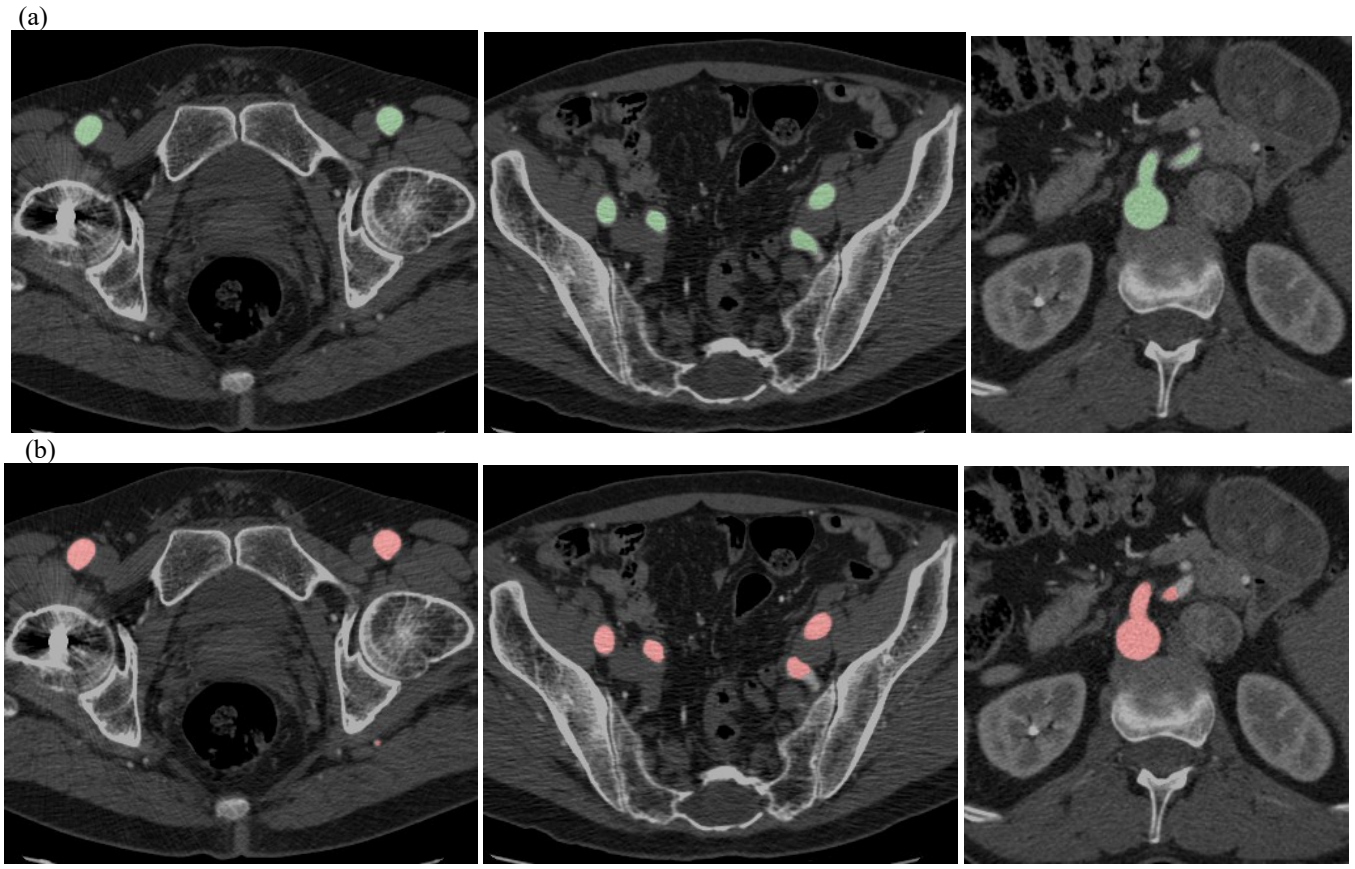

Fig. 3. (a) GT in green vs (b) UNet++ segmentation in red.

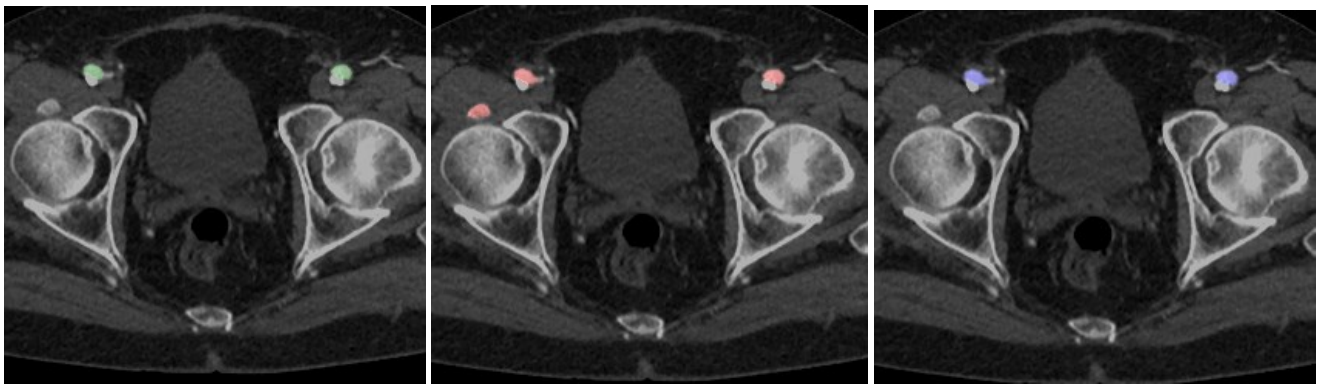

Fig. 4. Example of false positive filtered instance after post processing algorithm (a) ground truth (b) UNet++ segmentation (c) after post processing algorithm..

comprehensive approach allows for the analysis of the entire aortic morphology, particularly for planning endovascular aneurysm repair (EVAR).

The dataset was gathered from different collections and hospitals, exhibiting variations in resolution, and enabling the examination of the geometric and shape variabilities of human aortas and their branches across different geographic locations. The dataset provides a valuable resource for developing a robust statistical model of human aortic vessel tree shape, which can be utilized for the development of fully automated segmentation algorithms.

The evaluation of different backbone architectures for semantic segmentation networks demonstrates that Xception achieves superior performance in terms of accuracy and other evaluation metrics when compared to ResNet34, ResNet101, and VGG. These findings highlight the potential of Xception as a suitable choice for serving as the backbone architecture in semantic segmentation tasks [28].

Given the memory demands and larger dataset requirements of 3D convolutional neural networks (CNNs), some studies have focused on integrating orthogonal 2D CNNs for medical image segmentation [3], [29]. In our work, we introduce the post processing algorithm as a means to address spatial coherence, allowing for effective segmentation of the aorta and its branches in a coherent manner.

Overall, our proposed approach combines the power of deep learning and the incorporation of the post processing algorithm, enabling accurate and spatially coherent segmentation of the aorta to iliac arteries.

V. Future Work

- utilization of a larger dataset during model training to improve performance and mitigate overfitting.
- Increasing the diversity of the dataset by including CTA data from pre-operative and post-operative cases would further enhance the robustness of the trained model.
- This study focused specifically on the segmentation of contrast-enhanced CTA cases. However, the segmentation of non-contrast cases was not addressed, indicating the need for future investigation in this area.
- The influence of patient anatomy on segmentation outcomes was not explored in this research. However, with a larger test set, it would be possible to analyze how segmentation performance varies across different patient anatomies.
- While the proposed approach in this study focuses on segmenting the aortic lumen from CTAs, it does not encompass the segmentation of thrombus and calcifications. Additionally, as multi-class segmentation is more complex than binary segmentation, a more extensive dataset may be required to effectively train multi-class networks. Future research aims to incorporate the segmentation of thrombus and calcifications into the proposed approach.

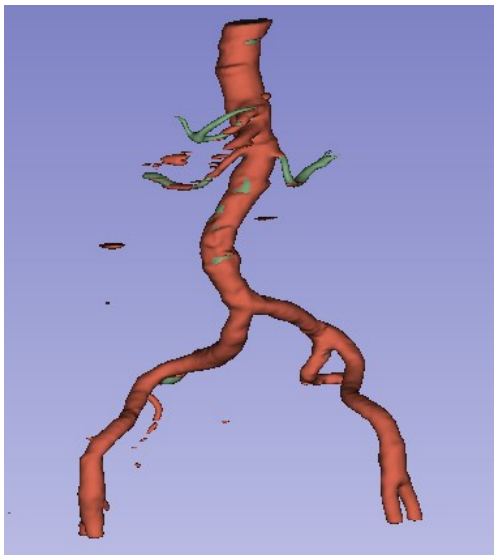

Fig. 5. 3D models generated from the ground truth and the automatic segmentations in green and red respectively the models are aligned together.

VI. Conclusion

The proposed automatic segmentation pipeline demonstrates promising results for morphology analysis, offering the potential to substantially reduce the workload for surgeons during the planning stage. The pipeline initially utilizes the UNet++ architecture for the segmentation task. Then, it enhances the segmentation results by incorporating the post processing algorithm, which ensures accurate segmentation of the branches and effectively eliminates false positive instances. This comprehensive approach facilitates the automatic segmentation of the abdominal aortic lumen and its branches, enabling various types of geometric analysis.

The automatic segmentation results also enable the generation of 3D models, which can be utilized for a wide range of numerical analyses. These analyses leverage the accurate and detailed 3D models obtained from the automatic segmentation, providing valuable insights and aiding in the planning and evaluation of surgical procedures.

References

[1] J. Golledge, "Abdominal aortic aneurysm: update on pathogenesis and medical treatments," Nat. Rev. Cardiol., vol. 16, no. 4, pp. 225–242, 2019, doi: 10.1038/s41569-018-0114-9.

[2] E. Altobelli, L. Rapacchietta, V. F. Profeta, and R. Fagnano, "Risk factors for abdominal aortic aneurysm in population-based studies: A systematic review and meta-analysis," Int. J. Environ. Res. Public Health, vol. 15, no. 12, 2018, doi: 10.3390/ijerph15122805.

[3] A. Fantazzini et al., "3D Automatic Segmentation of Aortic Computed Tomography Angiography Combining Multi-View 2D Convolutional Neural Networks," Cardiovasc. Eng. Technol., vol. 11, no. 5, pp. 576–586, 2020, doi: 10.1007/s13239-020-00481-z.

[4] A. Wanhainen et al., "Editor's Choice – European Society for Vascular Surgery (ESVS) 2019 Clinical Practice Guidelines on the Management of Abdominal Aorto-iliac Artery Aneurysms," Eur. J. Vasc. Endovasc. Surg., vol. 57, no. 1, pp. 8–93, 2019, doi: 10.1016/j.ejvs.2018.09.020.

[5] Z. H. Sun, "Abdominal aortic aneurysm: Treatment options, image visualizations and follow-up procedures," J. Geriatr. Cardiol., vol. 9, no. 1, pp. 49–60, 2012, doi: 10.3724/SP.J.1263.2012.00049.

[6] C. Kauffmann et al., "Measurements and detection of abdominal aortic aneurysm growth: Accuracy and reproducibility of a segmentation software," Eur. J. Radiol., vol. 81, no. 8, pp. 1688–1694, 2012, doi: 10.1016/j.ejrad.2011.04.044.

[7] S. Moccia, E. De Momi, S. El Hadji, and L. S. Mattos, "Blood vessel segmentation algorithms — Review of methods, datasets and evaluation metrics," Comput. Methods Programs Biomed., vol. 158, pp. 71–91, 2018, doi: 10.1016/j.cmpb.2018.02.001.

[8] M. de Bruijne, B. van Ginneken, M. A. Viergever, and W. J. Niessen, "Interactive segmentation of abdominal aortic aneurysms in CTA images," Med. Image Anal., vol. 8, no. 2, pp. 127–138, 2004, doi: 10.1016/j.media.2004.01.001.

[9] A. A. Duquette, P. M. Jodoin, O. Bouchot, and A. Lalande, "3D segmentation of abdominal aorta from CT-scan and MR images," Comput. Med. Imaging Graph., vol. 36, no. 4, pp. 294–303, 2012, doi: 10.1016/j.compmedimag.2011.12.001.

[10] F. Lareyre, C. Adam, M. Carrier, C. Dommerc, C. Mialhe, and J. Raffort, "A fully automated pipeline for mining abdominal aortic aneurysm using image segmentation," Sci. Rep., vol. 9, no. 1, pp. 1–14, 2019, doi: 10.1038/s41598-019-50251-8.

[11] S. Ghosh, N. Das, I. Das, and U. Maulik, "Understanding deep learning techniques for image segmentation," ACM Comput. Surv., vol. 52, no. 4, pp. 1–58, 2019, doi: 10.1145/3329784.

[12] A. Salvi, E. Finol, and P. G. Menon, "Convolutional Neural Network based Segmentation of Abdominal Aortic Aneurysms," Proc. Annu. Int. Conf. IEEE Eng. Med. Biol. Soc. EMBS, pp. 2629–2632, 2021, doi: 10.1109/EMBC46164.2021.9629499.

[13] F. Brutti et al., "Deep Learning to Automatically Segment and Analyze Abdominal Aortic Aneurysm from Computed Tomography Angiography," Cardiovasc. Eng. Technol., vol. 13, no. 4, pp. 535–547, 2022, doi: 10.1007/s13239-021-00594-z.

[14] G. Spinella et al., "Artificial Intelligence Application to Screen Abdominal Aortic Aneurysm Using Computed tomography Angiography," J. Digit. Imaging, no. 0123456789, 2023, doi: 10.1007/s10278-023-00866-1.

[15] Z. Zhou, M. M. Rahman Siddiquee, N. Tajbakhsh, and J. Liang, "Unet++: A nested u-net architecture for medical image segmentation," Lect. Notes Comput. Sci. (including Subser. Lect. Notes Artif. Intell. Lect. Notes Bioinformatics), vol. 11045 LNCS, pp. 3–11, 2018, doi: 10.1007/978-3-030-00889-5_1.

[16] E. Bousias Alexakis and C. Armenakis, "Evaluation of unet and unet++ architectures in high resolution image change detection applications," Int. Arch. Photogramm. Remote Sens. Spat. Inf. Sci. - ISPRS Arch., vol. 43, no. B3, pp. 1507–1514, 2020, doi: 10.5194/isprs-archives-XLIII-B3-2020-1507-2020.

[17] L. Radl et al., "AVT: Multicenter aortic vessel tree CTA dataset collection with ground truth segmentation masks," Data Br., vol. 40, p. 107801, 2022, doi: 10.1016/j.dib.2022.107801.

[18] J. Egger et al., "GBM volumetry using the 3D slicer medical image computing platform," Sci. Rep., vol. 3, pp. 1–7, 2013, doi: 10.1038/srep01364.

[19] P. Chlap, H. Min, N. Vandenberg, J. Dowling, L. Holloway, and A. Haworth, "A review of medical image data augmentation techniques for deep learning applications," J. Med. Imaging Radiat. Oncol., vol. 65, no. 5, pp. 545–563, 2021, doi: 10.1111/1754-9485.13261.

[20] A. Buslaev, V. I. Iglovikov, E. Khvedchenya, A. Parinov, M. Druzhinin, and A. A. Kalinin, "Albumentations: Fast and flexible image augmentations," Inf., vol. 11, no. 2, 2020, doi: 10.3390/info11020125.

[21] M. Cossio, "Augmenting Medical Imaging: A Comprehensive Catalogue of 65 Techniques for Enhanced Data Analysis," 2023, [Online]. Available: http://arxiv.org/abs/2303.01178

[22] F. Chollet, "Xception: Deep learning with depthwise separable convolutions," Proc. - 30th IEEE Conf. Comput. Vis. Pattern Recognition, CVPR 2017, vol. 2017-Janua, pp. 1800–1807, 2017, doi: 10.1109/CVPR.2017.195.

[23] S. Asgari et al., "Computerized Medical Imaging and Graphics Combo loss : Handling input and output imbalance in multi-organ segmentation," Comput. Med. Imaging Graph., vol. 75, pp. 24–33, 2019, doi: 10.1016/j.compmedimag.2019.04.005.

[24] A. A. Taha and A. Hanbury, "Metrics for evaluating 3D medical image segmentation: Analysis, selection, and tool," BMC Med. Imaging, vol. 15, no. 1, 2015, doi: 10.1186/s12880-015-0068-x.

[25] A. Paszke et al., "PyTorch: An imperative style, high-performance deep learning library. In Advances in Neural Information Processing Systems," NeurIPS, no. NeurIPS, pp. 8026–8037, 2019.

[26] K. López-Linares et al., "Fully automatic detection and segmentation of abdominal aortic thrombus in post-operative CTA images using Deep Convolutional Neural Networks," Med. Image Anal., vol. 46, pp. 202–214, 2018, doi: 10.1016/j.media.2018.03.010.

[27] K. López-Linares, I. García, A. García-Familiar, I. Macía, and M. A. G. Ballester, "3D convolutional neural network for abdominal aortic aneurysm segmentation," 2019, [Online]. Available: http://arxiv.org/abs/1903.00879

[28] R. Zhang, L. Du, Q. Xiao, and J. Liu, "Comparison of Backbones for Semantic Segmentation Network," J. Phys. Conf. Ser., vol. 1544, no. 1, 2020, doi: 10.1088/1742-6596/1544/1/012196.

[29] J. Noothout, B. de Vos, J. Wolterink, and I. Isgum, "Automatic segmentation of thoracic aorta segments in low-dose chest CT," p. 63, 2018, doi: 10.1117/12.2293114.